

SUPERCONDUCTIVITY-BASED ARTIFICIAL ATOMS FOR QUANTUM INFORMATION

BY ALEXANDRE BLAIS

One hundred years after its discovery, superconductivity keeps surprising the physics community. One of these surprises came five years after the seminal BCS paper. Then, a 22 year-old PhD student, Brian Josephson, made the bold prediction that a dissipation-less current, a supercurrent, would flow through two superconductors separated by a thin insulating barrier^[1]. This prediction was met with great skepticism by John Bardeen, who believed that electrons across the insulating barriers would not be correlated, thereby preventing any significant supercurrent flow^[2]. Josephson received the Nobel prize in 1973, ten years after the experimental confirmation of what is now known as the Josephson effect^[3] and only one year after Bardeen, Cooper, and Schrieffer's Nobel prize.

Over the years, the Josephson effect has developed as a versatile tool for fundamental science and has found many applications. For example, Josephson junctions can be used to redefine the volt standard, and can be incorporated in superconducting quantum interference devices (SQUIDs) to make sensitive magnetometers^[4]. In the mid-eighties, it also became clear that electrical circuits based on Josephson junctions could behave as artificial atoms under well controlled experimental conditions^[5]. By this, it is meant that the circuit is well described by quantized energy levels whose separation is larger than thermal energy $k_B T$. The system must also be sufficiently decoupled from uncontrolled degrees of freedom (the environment) for its lifetime T_1 to be large.

Before considering the quantum mechanics of Josephson junctions, it is instructive to review a well known case, the LC oscillator illustrated in Fig. 1a). It is characterized by

SUMMARY

Electrical circuits based on Josephson junctions, the only known nonlinear and nondissipative circuit element, can behave as artificial atoms with well defined energy levels whose separation exceeds thermal energy. These man-made atoms are now being used in several labs worldwide to realize simple quantum processors and attain new regimes of quantum optics.

the angular frequency $\omega_0 = \sqrt{1/LC}$ and the characteristic impedance $Z_0 = \sqrt{L/C}$. R_{int} represents internal losses, while the combination C_{ext} and R_{ext} is a minimal model representing outside circuitry used to interact with the LC . In a quantum description and excluding dissipation for the moment, the conjugate variables Q (the charge on the capacitor) and Φ (the flux threading the inductor) entering the classical energy of the circuit

$$H_{LC} = \frac{Q^2}{2C} + \frac{\Phi^2}{2L} \quad (1)$$

are promoted to non-commuting operators: $Q \rightarrow \hat{Q} = i\sqrt{\hbar/2Z_0}(\hat{a}^\dagger - \hat{a})$, $\Phi \rightarrow \hat{\Phi} = \sqrt{\hbar Z_0/2}(\hat{a}^\dagger + \hat{a})$. We have introduced the standard creation (\hat{a}^\dagger) and annihilation (\hat{a}) operators of the harmonic oscillator, which of course lead to $H_{LC} = \hbar\omega_0 \hat{a}^\dagger \hat{a}$. Here, \hat{a}^\dagger creates quantized excitations of the electromagnetic field in the oscillator, or more simply said photons at frequency ω_0 .

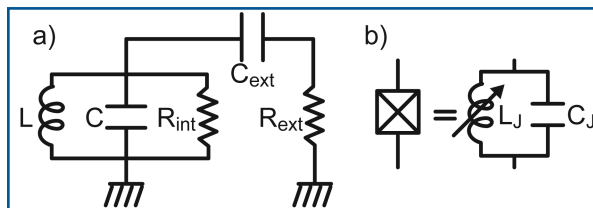


Fig. 1 a) Harmonic oscillator with internal and external losses. b) Circuit representation of a Josephson junction and its equivalent circuit: the parallel combination of a nonlinear inductor L_J and a capacitor C_J .

In this context, the conditions of well defined energy levels mentioned above translate to $\hbar\omega_0 \gg k_B T$, while for the lifetime the standard result $T_1 = RC$ is obtained, where $R = 1/\text{Re}[Y(\omega)]$ with $Y(\omega)$ the admittance of the electromagnetic environment of the LC composed of R_{int} , R_{ext} and C_{ext} ^[6]. With standard microfabrication techniques, values of $L \sim 0.1$ nH and $C \sim 1$ pF can be obtained, leading to frequencies in the microwave regime $\omega_0/2\pi \sim 16$ GHz. Given that $1 \text{ GHz} \times \hbar/k_B \sim 50$ mK, the condition $\hbar\omega_0 \gg k_B T$ can easily be satisfied in a dilution refrigerator operating at 20 mK. On the other hand, the condition of minimal losses can be satisfied by working with superconducting materials (typically Al or Nb) and reducing the coupling to the external world.



A. Blais
<a.blais@usherbrooke.ca>, Département de Physique, Université de Sherbrooke, Sherbrooke, QC, J1K 2R1

et membre des programmes Matériaux quantiques, Information quantique et Nanoélectronique, Institut canadien de recherches avancées, Toronto, ON, M5G 1Z8

While a superconducting LC circuit can be described accurately as an artificial atom with discrete energy levels, showing bona fide quantum behavior is challenging. Indeed, the harmonic oscillator is always in the correspondence limit and some amount of nonlinearity is required to break away from this. This is where Josephson junctions enter. These junctions are the only known nonlinear and nondissipative circuit elements. They have vanishing internal losses because a supercurrent, not a normal current, flows through the junction. Moreover, the nonlinearity can be understood from Josephson's relations which we now discuss.

In his seminal paper, Josephson obtained two main relations governing the dynamics of Josephson junctions^[1]. First, he showed that the current I flowing through a junction is related to the difference of phase ϕ between the two superconductors forming the junction: $I = I_c \sin \phi$. In this expression, I_c is the maximum current that can be pushed through the junction before breaking Cooper pairs. The second Josephson relation relates ϕ to the voltage across the junction: $\dot{\phi} = 2eV/\hbar$. These two relations can be combined to obtain $I = I_c \sin(2\pi\Phi/\Phi_0)$, where $\Phi = \int dtV(t)$ is a flux and $\Phi_0 = h/2e$ the flux quantum. This relation relates current to flux, just as the constitutive relation of an inductor does. It is then useful to define the Josephson inductance $L_J = (\partial I/\partial \Phi)^{-1} = \Phi_0/(2\pi I_c \cos(2\pi\Phi/\Phi_0))$, a *nonlinear* function of Φ . As illustrated in Fig. 1b), a Josephson junction can thus be modeled by the parallel combination of a capacitor C_J (the two superconducting electrodes separated by an oxide barrier) and a nonlinear inductor L_J , forming a nonharmonic oscillator whose energy levels will not only be discrete but nonlinearly spread. Experimental confirmation of these predictions have been obtained in the mid-eighties in groundbreaking work from J. Clarke's group at Berkeley^[5].

To better understand how a Josephson junction acts as a nonlinear oscillator, it is instructive to consider the energy related to pair tunneling. This is obtained simply by noting that the energy stored in the junction is $E = \int dtV(t)I(t) = -E_J \cos(2\pi\Phi/\Phi_0)$ where we have again used the two Josephson relations and have introduced $E_J = \Phi_0 I_c/2\pi$, the Josephson energy. Similarly to the simple LC oscillator, the junction Hamiltonian then reads

$$H_J = \frac{Q^2}{2C_J} - E_J \cos(2\pi\Phi / \Phi_0). \tag{2}$$

Quantizing the macroscopic variables Q and Φ , and again doing the replacement in terms of $\hat{a}^{(\dagger)}$ yields, after expanding the cosine to fourth order (a good approximation for large E_J) and neglecting fast oscillating terms,

$$H_J \approx \hbar\omega_J \hat{a}^\dagger \hat{a} + \hbar\chi(\hat{a}^\dagger \hat{a})^2, \tag{3}$$

where $\omega_J \approx \sqrt{8E_C E_J}$ and $\chi = -E_C/2$, with $E_C = e^2/2C_J$ the energy cost to adding a charge on the junction capacitance, also called charging energy. In quantum optics, this Hamiltonian is well known to describe nonlinear Kerr media^[7]. Because the spectrum of \hat{H}_J is nonlinear, it is possible to use the first two

levels $\{|0\rangle, |1\rangle\}$ as logical states of a qubit, or in an alternative but equivalent picture, as the first two levels of an artificial atom^[8].

But what are the advantages of these artificial atoms with respect to genuine ones? For one, atoms have much longer lifetimes than their artificial counterparts. For example, hyperfine states of $^9\text{Be}^+$ used for ion trap quantum computing have for all practical purposes infinite relaxation time T_1 and coherence time T_2 , representing the time over which phase information in a superposition of basis states $\{|0\rangle, |1\rangle\}$ is preserved, exceeding 10 seconds^[9]. With the typical time to control the quantum states of these ions of the order of a few microseconds, there is ample time for realizing high-fidelity quantum gates. As a result, the error per gate can be quite low, of the order of 0.48 %^[10]. On the other hand, T_1 for superconducting qubits is typically a few *microseconds* and $T_2 \sim 2T_1$ or shorter^[11]. While this could appear disastrous, it is outweighed by the fast operation time in the solid-state. Indeed artificial atoms have low T_1 because they are big (literally) resulting in a large dipole moment and thus strong coupling to electric field. While uncontrolled coupling leads to relaxation, this also allows for fast operations. Using optimal control techniques^[12], it is indeed possible to realize single-qubit gates with precisely controlled bursts of voltage in as little as 4 ns^[13]. The resulting error per gate of 0.7 % is approaching trapped ions results^[10].

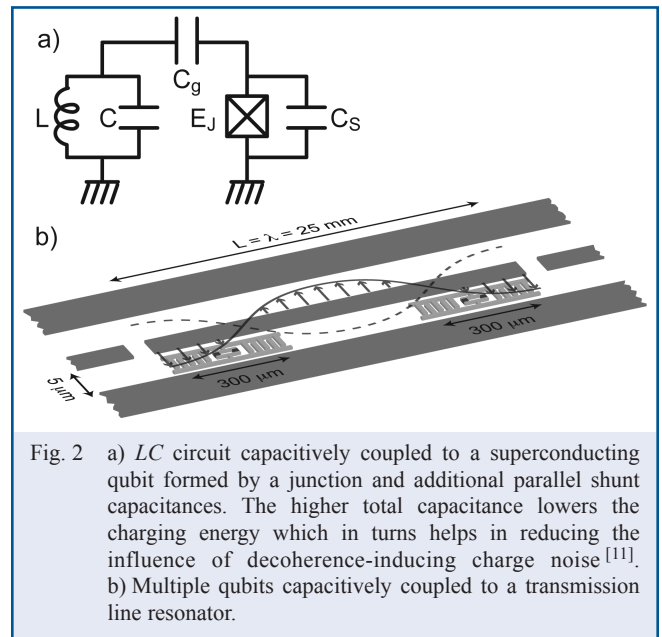


Fig. 2 a) LC circuit capacitively coupled to a superconducting qubit formed by a junction and additional parallel shunt capacitances. The higher total capacitance lowers the charging energy which in turns helps in reducing the influence of decoherence-inducing charge noise^[11]. b) Multiple qubits coupled to a transmission line resonator.

In addition to having a large dipole moment, superconducting electrical circuits can also show large quantum fluctuations of the voltage. Consider for example the superconducting qubit capacitively coupled to a LC oscillator illustrated in Fig. 2a). In its ground state (easily reached at dilution fridge temperatures), the average voltage $\langle \hat{V} \rangle = \langle \hat{Q}/C \rangle$ across the LC is zero. Zero-point fluctuations are however quite large,

$\sqrt{\langle \hat{V}^2 \rangle} = \sqrt{\hbar\omega_0 / 2C} \sim 2\mu\text{V}$ for the parameters given above. This leads to strong electric-dipole coupling between the (artificial) atom and the microwave photons that are the excitations of the LC^[14]. This situation is more typically realized in cavity quantum electrodynamics, where Rydberg atoms are sent one by one through a pair of mirrors forming a cavity^[15]. In circuits however, because of the unique combination of large dipole moment and large zero-point voltage, the light-matter interaction can be orders of magnitude stronger^[16], leading to a host of novel effects^[17,18]. This solid-state realization of cavity QED is known as circuit QED.

Circuit QED can also be used for quantum information processing. Indeed, in practice and as illustrated in Fig. 2b), the LC can be realized by a ~ 1 cm long high-Q transmission line resonator^[16,19]. Since it is possible to couple several qubits to a single resonator, it can serve as a quantum bus mediating

interactions between remote qubits. With the high-fidelity quantum gates mentioned above, circuit QED has been used to implement simple two-qubit quantum algorithms^[20] and to entangle three qubits^[21,22]. Beyond quantum information processing, circuit QED and artificial atoms also open new possibilities for quantum optics and this is only now starting to be explored in the laboratory. Notable realizations are on-demand single microwave photon sources^[23] and the subsequent demonstration of microwave photon anti-bunching, a clear signature of the quantum nature of these microwave excitations^[24]. Given the pace at which this field is moving, the future prospects of Josephson junction based artificial atoms look rather good.

ACKNOWLEDGEMENTS

Support from NSERC, the Alfred P. Sloan Foundation and CIFAR is acknowledged.

REFERENCES

1. B.D. Josephson, *Physics Letters* **1**, 251 (1962).
2. J. Bardeen, *Phys. Rev. Lett.* **9**, 147 (1962).
3. P.W. Anderson and J.M. Rowell, *Phys. Rev. Lett.* **10**, 230 (1963).
4. J. Clarke and A.I. Braginski, *The SQUID Handbook: Fundamentals and Technology of SQUIDS and SQUID Systems*, Wiley-VCH, (2004).
5. J. Clarke, A.N. Cleland, M. Devoret, D. Esteve, and J. Martinis, *Science* **992**, 239 (1988).
6. D. Esteve, M.H. Devoret, and J.M. Martinis, *Phys. Rev. B* **34**, 158 (1986).
7. D. Walls and G.J. Milburn, *Quantum Optics*, Springer, Berlin, (2008), 2 ed.
8. A. Zagoskin and A. Blais, *Physics in Canada* **63**, 215 (2007).
9. C. Langer, R. Ozeri, J.D. Jost, J. Chiaverini, B. DeMarco, A. Ben-Kish, R.B. Blakestad, J. Britton, D.B. Hume, W.M. Itano, D. Leibfried, R. Reichle, T. Rosenband, T. Schaetz, P.O. Schmidt, and D.J. Wineland, *Phys. Rev. Lett.* **95**, 060502 (2005).
10. For a comparison of the relative performance of various qubits, see Table 1 of T.D. Ladd, F. Jelezko, R. Laflamme, Y. Nakamura, C. Monroe, and J.L. O'Brien, *Nature* **464**, 45 (2010).
11. A. Houck, J. Koch, M. Devoret, S. Girvin, and R. Schoelkopf, *Quantum Information Processing* **8**, 105 (2009).
12. F. Motzoi, J.M. Gambetta, P. Rebentrost, and F.K. Wilhelm, *Phys. Rev. Lett.* **103**, 110501 (2009).
13. J.M. Chow, L. DiCarlo, J.M. Gambetta, F. Motzoi, L. Frunzio, S.M. Girvin, and R.J. Schoelkopf, *Phys. Rev. A* **82**, 040305 (2010).
14. In the presence of the oscillator, the charge \hat{Q}_q on the qubit in Eq. (2) is replaced by $\hat{Q}_q - \hat{Q}_q + C_g \hat{Q}_{LC} / (C_g + C_J + C_S)$, where \hat{Q}_{LC} is the charge on the LC. This leads to coupling $\propto \hat{Q}_q \hat{Q}_{LC}$ between the 'atom' \hat{Q}_q and 'photons' \hat{Q}_{LC} .
15. S. Haroche and J.-M. Raimond, *Exploring the Quantum: Atoms, Cavities, and Photons*, Oxford University Press, Oxford, (2006).
16. A. Blais, R.-S. Huang, A. Wallraff, S.M. Girvin, and R.J. Schoelkopf, *Phys. Rev. A* **69**, 062320 (2004).
17. R.J. Schoelkopf and S.M. Girvin, *Nature* **451**, 664 (2008).
18. S.M. Girvin, M.H. Devoret, and R.J. Schoelkopf, *Physica Scripta* **T137**, 014012 (13pp) (2009).
19. A. Wallraff, D.I. Schuster, A. Blais, L. Frunzio, R.-S. Huang, J. Majer, S. Kumar, S.M. Girvin, and R.J. Schoelkopf, *Nature* **431**, 162 (2004).
20. L. DiCarlo, J.M. Chow, J.M. Gambetta, L.S. Bishop, B.R. Johnson, D.I. Schuster, J. Majer, A. Blais, L. Frunzio, S.M. Girvin, and R.J. Schoelkopf, *Nature* **460**, 240 (2009).
21. L. DiCarlo, M.D. Reed, L. Sun, B.R. Johnson, J.M. Chow, J.M. Gambetta, L. Frunzio, S.M. Girvin, M.H. Devoret, and R.J. Schoelkopf, *Nature* **467**, 574 (2010).
22. M. Neeley, R.C. Bialczak, M. Lenander, E. Lucero, M. Mariantoni, A.D. O'Connell, D. Sank, H. Wang, M. Weides, J. Wenner, Y. Yin, T. Yamamoto, A.N. Cleland, and J.M. Martinis, *Nature* **467**, 570 (2010).
23. A.A. Houck, D.I. Schuster, J.M. Gambetta, J.A. Schreier, B.R. Johnson, J.M. Chow, L. Frunzio, J. Majer, M.H. Devoret, S.M. Girvin, and R.J. Schoelkopf, *Nature* **449**, 328 (2007).
24. D. Bozyigit, C. Lang, L. Steffen, J.M. Fink, C. Eichler, M. Baur, R. Bianchetti, P.J. Leek, S. Filipp, M.P. da Silva, A. Blais, and A. Wallraff, *Nat Phys* **7**, 154 (2011).